

rijkswaterstaat

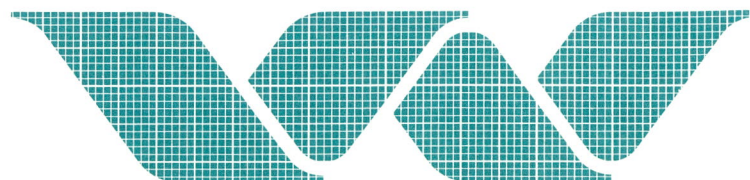
dienst getijdewateren

nr. C-1414, 351

bibliotheek

515

DI: 63438



waterloopkundig laboratorium delft hydraulics laboratory

Some first particle track computations with fine
grid and coarse grid velocity fields of the Southern
North Sea

H. Gerritsen

Publication No.351

September 1985

Some first particle track computations with fine
grid and coarse grid velocity fields of the Southern
North Sea

Presented at the Colloquium on Computation of
Tracks and Distributions of Particles in 2- and
3-dimensional velocity fields,
The Hague, June 19, 1985

H. Gerritsen

Publication No. 351

September 1985

Some first particle track computations with fine grid and coarse grid velocity fields of the Southern North Sea.

by
Herman Gerritsen^{*)}

Abstract:

In this paper a recently developed particle track simulation model is presented. Various aspects are discussed, and numerical errors due to discretization, interpolation and time-integration are estimated. Its capabilities are illustrated on two applications in ongoing research. The first is taken from a study of the influence of small scale bottom topography in the North Sea on the representation of transport of matter using numerical models. In the second illustration particle track computations are performed in a comparison of several tide-averaged velocity concepts with respect to their usefulness in long term transport simulations.

1 Introduction

The Southern part of the North Sea is a funnel-shaped shallow water area which is connected to the English Channel by means of the narrow Dover Straits passage. It is characterized by an indented estuarine coast with large river inflows and a semidiurnal tide of resonance type with tidal amplitudes over 1 meter, increasing to 4 meters near Dover Straits.

There is a steady input of pollution both from rivers such as Scheldt, Thames and Rhine, and from regular dumping activities at open sea. For the assessment of the long term effects of these and other ecological hazards a good understanding of the behaviour of passive matter in the area is needed.

Computer modelling of flows and transports supplies a flexible set of tools with which insight into the behaviour of the system under various circumstances can be obtained. In this paper a numerical model is presented in which the positions and tracks of passive tracer particles are determined. This particle track model is presently being developed at the Delft Hydraulics Laboratory as a general research tool. The advective transport by the pres-

^{*)} Delft Hydraulics Laboratory/Waterloopkundig Laboratorium, Delft - NL

cribed (tidal or steady) flow can be fully simulated; diffusive spreading has as yet not been incorporated in the model. The capabilities of the model are illustrated in two applications in ongoing research, each giving rise to some interesting results.

In section 2 a description of the particle track model and its implementation characteristics is given. Some attention is also given to numerical error sources such as discretization, interpolation, and time-integration. Section 3 presents an application in which the influence on the particle tracks of small scale topographic features in the North Sea is studied. In section 4 a comparison of several tide-averaged velocity concepts is made, showing that the mean track velocity may form an accurate and most effective velocity concept for the longer time scales. Finally, in section 5 some conclusions are drawn.

2 The particle track computation model

Conceptually a particle track computation model is simple: on the basis of a given steady velocity field, or a series of (cyclic) time-dependent velocity fields, the position in time of one or more particles is determined, starting from prescribed initial positions. The corresponding differential equation for the particle motion is:

$$\frac{d\vec{X}(t)}{dt} = \vec{U}_{\text{prescr}}(\vec{X}, t) \quad (2.1)$$

Its solution is given by:

$$\vec{X}(t) = \vec{X}(t=0) + \int_0^t \vec{U}_{\text{prescr}}(\vec{X}(t'), t') dt' \quad (2.2)$$

X and U are functions of 1, 2 or 3 spatial variables. The computation can be performed off-line, as a post processing operation to the flow computation, since the particles are assumed to be passive: they are moved by the flow but in turn do not influence the water motion (no dynamical interaction).

The equation (2.1) above represents the advective transport. Addition of a small stochastic component to \vec{U} to account for diffusion is not considered here.

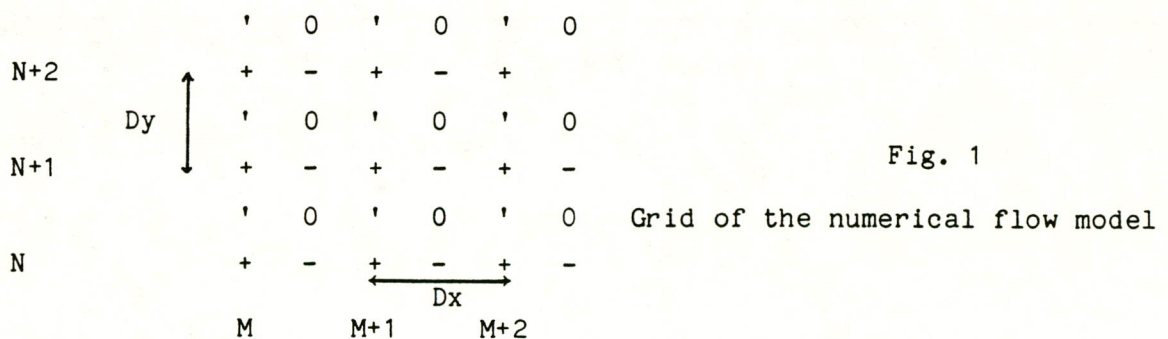
The solution Eq. 2.2 is implemented for the case of flow in two dimensions.

This may be either depth-integrated (horizontal) flow, or width-integrated flow. The program package has a modular structure. The inclusion of a diffusion module at a later stage is therefore straightforward and simple. Eq. 2.1 is solved using either a first or second order time-stepping scheme, with fixed time step Δt . Various plot facilities to present the results, either as tracks of individual particles, or as patches of particles, have been incorporated. In the following sections several aspects of the program modules are discussed:

- interpolation of the velocities on the grid of the hydrodynamic flow computation
- solution of Eq. 2.1 near closed boundaries
- particle discharge options
- withdrawal of particles at open boundaries
- numerical error sources.

Interpolation in the velocity grid

Many applications of the particle track model will be to situations of horizontal flow, with hydrodynamic flow input obtained from the WAQUA flow model in use by the Ministry of Transport and Public Works and the Delft Hydraulics Laboratory, [5]. Fig. 1 shows the grid used in the flow computation (gridsize $Dx = Dy$):



The grid is staggered in space, with the following position definitions:

+	: water levels	$\zeta(N,M)$	~	$\zeta(NDy, MDx)$
-	: u-velocities	$u(N,M)$	~	$u(NDy, (M+\frac{1}{2})Dx)$
+	: v-velocities	$v(N,M)$	~	$v((N+\frac{1}{2})Dy, MDx)$
0	: depths	$H(N,M)$	~	$H((N+\frac{1}{2})Dy, (M+\frac{1}{2})Dx)$

The values of u , v and ζ are determined at each half of the time step Dt of

the flow computation, which is of overall second order accuracy. To determine a velocity component at an arbitrary position during the track computation, bilinear interpolation between the four nearest corresponding velocity grid points is used.

Solution near closed boundaries

All information on the location of the closed boundaries is contained in the velocity fields. Although normal velocities vanish at the boundary, the straightforward application of the discretized version of Eq. 2.2 for given time-step Δt of the particle track computation may result in a displacement across the boundary. To prevent this a special implementation is used near closed boundaries, which is based on reflection according to Snell's law. For a correct application of this procedure, in which the possible vanishing of all four velocity values around the nearest depth position is taken into account, it is required that Δt is bounded by:

$$\Delta t \leq \frac{\Delta x}{2 \max_{x,y,t} |\vec{u}|} \quad (2.3)$$

Whenever a particle reaches the closed boundary it moves further along the boundary, since in the case of advective transport only, which is considered here, there is no agent (e.g. diffusion) which may bring the particle back into the interior flow field.

Particle discharge options

Three options have been implemented:

- initial discharges of particles at n prescribed positions X_n , with single discharges at positions X_m after $k(m)$ time steps, and periodic discharges at positions X_l each $k(l)$ time steps;
- initial discharge of m times n particles evenly distributed on the circumference of m circles with given radius and center position;
- initial discharge of one particle in each m -th waterlevel grid point in both spatial directions.

These options cover most cases of practical interest (Note that the simultaneous discharge of several particles at one single position will result in identical tracks since no initial diffusion or other artificial spreading mechanism is applied).

Withdrawal at open boundaries

Open boundary zones can be defined if needed. Particles are withdrawn when they enter these zones. Once removed, the particles cannot be reintroduced into the simulation.

Numerical error sources

In the numerical solution of the equation three possible error sources should be taken into account. These will be illustrated on the one-dimensional case with variation in x and t only:

- the integration procedure

Two straightforward integration techniques are considered:

A. Forward Euler time stepping; time step Δt

Denoting the numerical representation of the differential equation by

$$F_{\text{num}} = \frac{x^{n+1} - x^n}{\Delta t} - u(x(t^n), t^n), \quad (2.4)$$

one obtains for the difference with the analytical solution:

$$(F_{\text{num}} - F_{\text{an}}) \Big|_{t=t^n} = \frac{\Delta t}{2!} \frac{d^2 x}{dt^2} + O(\Delta t^2), \quad (2.5)$$

i.e. a first order accurate solution.

B. Predictor-corrector; second order in time:

$$\bar{x}^{n+1} = x^n + \Delta t [u(x^n(t^n), t^n)]$$

$$x^{n+1} = x^n + \frac{\Delta t}{2} [u(x^n(t^n), t^n) + u(\bar{x}^{n+1}(t^{n+1}), t^{n+1})] \quad (2.6)$$

With

$$F_{\text{num}} = \frac{x^{n+1} - x^n}{\Delta t} - \frac{1}{2} [u(x(t^n), t^n) + u(\bar{x}^{n+1}, t^{n+1})], \quad (2.7)$$

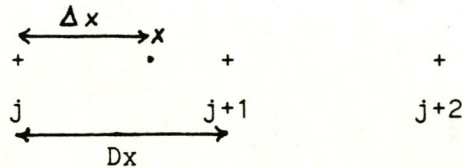
one now obtains:

$$(F_{\text{num}} - F_{\text{an}})_{t=t^{n+1/2}} = \frac{\Delta t^2}{8} \left(\frac{d^2 u}{dt^2} + u^2 \frac{\partial^2 u}{\partial x^2} \right) + \frac{\Delta t^2}{24} \frac{d^3 u}{dt^3} + O(\Delta^3), \quad (2.8)$$

i.e. a second order accurate solution.

- discretization/interpolation in space

The horizontal velocity fields u and v are only known on a fixed grid with grid sizes Dx and Dy . In one dimension the bilinear interpolation used to determine velocity values in arbitrary particle positions (x,y) reduces to linear interpolation in u , known at gridpoints Dx apart, see sketch:



So, $u(x)$ is replaced by:

$$u(jDx) + \frac{\Delta x}{Dx} \{u((j+1)Dx) - u(jDx)\} \quad (2.9)$$

This introduces the formally first order error:

$$\Delta x(Dx - \Delta x) \left[\frac{1}{2!} \frac{d^2 u}{dx^2} + \frac{(Dx - 2\Delta x)}{3!} \frac{d^3 u}{dx^3} + \frac{Dx \cdot Dx - 5Dx \cdot \Delta x + 5\Delta x \cdot \Delta x}{4!} \frac{d^4 u}{dx^4} + \dots \right], \quad (2.10)$$

since in general $Dx \neq \Delta x$. Often one has:

$$Dx \gg \Delta x \quad (2.11)$$

Note. A choice $\Delta x = Dx$ is not possible since with a fixed value for Δt the solution of Eq. (2.2) determines the local value of Δx .

- choice of the time step

Consider the case of time-dependent velocity input.

Let Dt denote the time interval at which the velocity fields u and v are known; Dt generally is the time step in the solution of the shallow water equations. Since the time step Δt in the solution of Eq. (2.1) does not necessarily have to be equal to Dt , an interpolation in time may be necessary to determine the velocity at the particle position at the time t . In the case of linear interpolation between two time levels, the error due to interpolation of the velocity u in time is analogous to (2.10) and reads:

$$\Delta t(Dt - \Delta t) \left[\frac{1}{2!} \frac{d^2 u}{dt^2} + \frac{(Dt - 2\Delta t)}{3!} \frac{d^3 u}{dt^3} + \dots \right] \quad (2.12)$$

A similar error holds for the interpolation of v -values in time.

Note that these errors fully disappear if one chooses $\Delta t = Dt$.

From the error sources it is clear that a fully second order solution of Eq. (2.1) is not possible if bilinear interpolation in space is used. In particle track computations with time-dependent flow fields the error in time is determined both by the choice of solver and the choice of Δt in relation to Dt . This leads to the paradox that reducing the time step Δt below Dt may very well lead to less accurate results since fully second order solution in time can only be realized with a second order solver in combination with $\Delta t = Dt$.

3 Application 1: Fine grid versus coarse grid particle tracks

In [1], Abraham and Lindijer investigated the influence of sub-grid scale processes on the representation of the flow in numerical models. As part of their study they compared flow results obtained with a coarse grid (10,000 m) model with results of a fine grid (1500 m) model, the latter results having been averaged to the scale of the coarse grid. Significant differences were found for areas with, and areas without small scale bottom topography (Figs. 2 and 3), see [1] for further details. The present example is taken from the follow up of this study. In order to investigate whether the studied feature also holds for the transport of matter, four relatively simple particle track computations were performed.

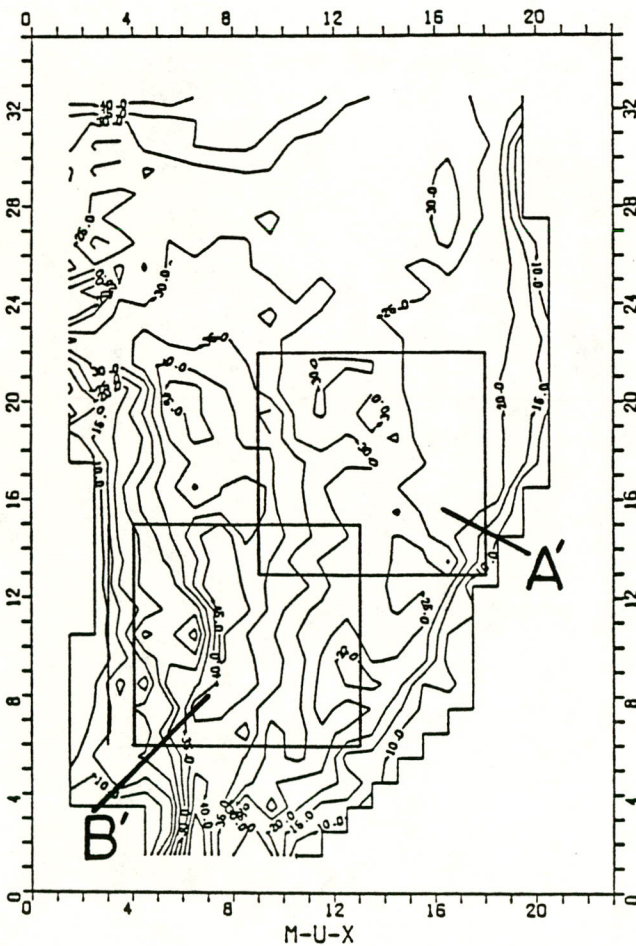


Fig. 2. Depth contours in the coarse grid
Southern North Sea flow model
(Dx = 10,000 m)

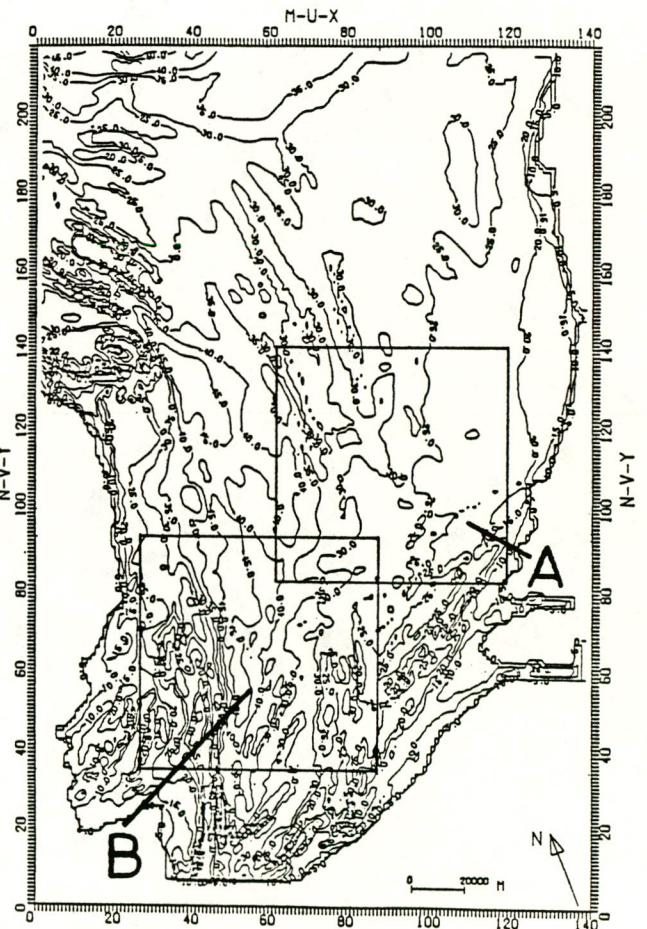


Fig. 3. Depth contours in the fine grid
Southern North Sea flow model
(Dx = 1500 m)

In the model region, two $90 \times 90 \text{ km}^2$ areas A and B are defined, see Fig. 3. Area B is characterized by intense small scale bottom topography, while area A is relatively smooth. The corresponding areas in the coarse grid are denoted by B' and A', respectively. From Fig. 2 it is seen that the strong topographic variations in B ($\Delta x = 1500 \text{ m}$) have a largely sub-grid scale character in area B' ($\Delta x = 10,000 \text{ m}$): they cannot be sufficiently represented on this larger scale.

In both coarse grid areas A' and B' three initial patches are defined. Each patch is described by the locations of 40 particles uniformly distributed on the circumference of a circle with a prescribed radius. At the corresponding locations in the fine grid areas A and B identical patches are defined. The solution of Eq. 2.2 in time for each particle starting from these initial circular distributions, yields information on the development with time of the size and form of the patches. The velocity input u and v is provided by the available results of the coarse grid and fine grid flow simulations, see [1]. For a description of the parameters in the flow computations, see Table I.

Type of grid:	coarse (A,B)	fine (A',B')
Bottom topography	Fig. 2	Fig. 3
Grid size in meters	10.000	1.500
Period of cyclic tide (minutes)	750	750
Time-step Δt in minutes	10	5
Cyclic period used:	8th	8th
Overall accuracy of the results:	2nd order	2nd order

Table I: Characteristics of the flow computations

The circle diameter was chosen to be 18 km, which corresponds to 1.8 and 12 times the grid sizes in the coarse and fine grids, respectively. The initial patch size is then sufficiently large in order that the inhomogeneities in the

velocity fields can effectuate the correct advective spreading of the patches directly from the start of the simulation.

The further details of the track computations are given in Table II.

type of computation	coarse grid (10000 m)		fine grid (1500 m)	
area	A'	B'	A	B
type of bottom topography	relatively flat area	sub-grid scale topography	relatively smooth	small scale bottom topography
number of initial circles	3	3	3	3
number of particles per circle	40	40	40	40
circle radius - in km	18	18	18	18
- in grid size	1.8	1.8	12	12
time step Δt (minutes)	10 (= DT)	10 (= DT)	5 (= Dt)	5 (= Dt)
duration of the simulation	1500 hrs	1500 hrs	750 hrs	750 hrs
- order of the solution method	1st	1 st	1 st	1 st
- interpolation of the velocities:				
- in space	bilinear	bilinear	bilinear	bilinear
- in time	none	none	none	none

Table II: Characteristics of the track computations

Figs. 4 and 5 show the results of the coarse grid particle track computations for the initial particles in areas A' and B'. The deformation and size of the patches have been made visible by connecting each particle to its neighbour from the initial circle circumference. The resulting patches are shown for $t = 0$ to $t = 1500$ hours for B', and to 1300 hours for A', at intervals of 100 hours.

The mean direction of the transport is Northward. The net displacement of the patches in 1500 hrs corresponds to net mean velocities between 2.5 cm/sec. (near the Dutch coast) and 6 cm/sec (more near the center of the region). The smaller patch deformations in area A' reflect the fact that the velocity variations are relatively smooth, which in turn is related to the comparatively flat bottom topography in the area. (Note that this does not exclude velocity variations as such!). The three patches in area B' show much larger deformations, which is caused by the more complex bottom topography (Fig. 3), resulting in a finer velocity structure. This causal relation is borne out most explicitly by the strong deformation of the left most patch.

For computational efficiency the u and v velocities of the $90 \times 90 \text{ km}^2$ fine grid areas A and B were first extracted from the full velocity fields. The patches could consequently be followed only within the pertaining area of 60×60 grid boxes.

Figs. 6 and 7 show the results at 100 hour intervals in area A (relatively smooth bottom topography) and B (strong topographic variations), respectively. Simply because of the smaller grid size the patch development in area A shows much more detail than that in area A': the inhomogeneities in the flow field are now more effective in the small scale spreading. These differences are not fundamental, however. A not too drastic smoothing of the patch boundaries results in patches which are largely comparable to those of Fig. 4. In other words: the large scale effect of sub-grid scale bottom topography in relatively flat areas such as A' and A is only small.

Comparison of Figs. 7 and 5 shows that the situation is different for the

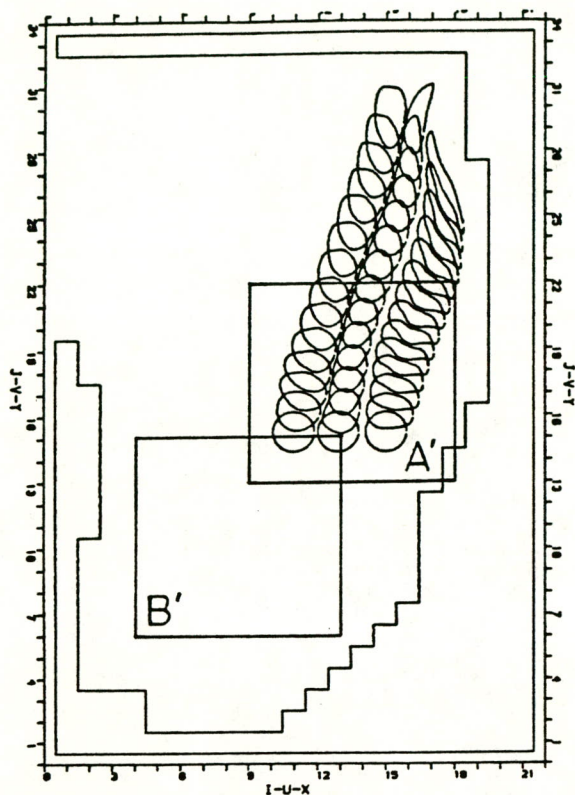


Fig. 4. Positions of the particle patches released in the relatively flat area A' in the coarse grid at intervals of 100 hrs between $T = 0$ and $T = 1300$ hrs

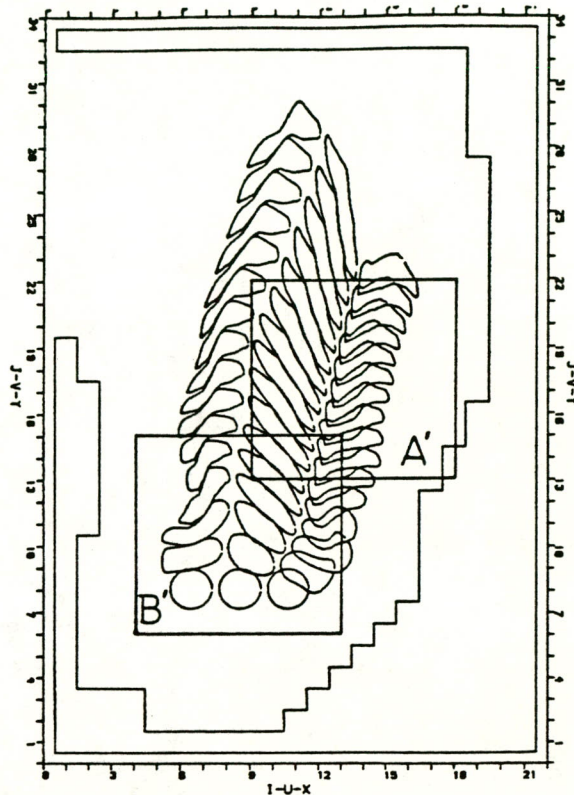


Fig. 5. Positions of the particle patches released in area B' in the coarse grid at intervals of 100 hrs between $T = 0$ and $T = 1500$ hrs

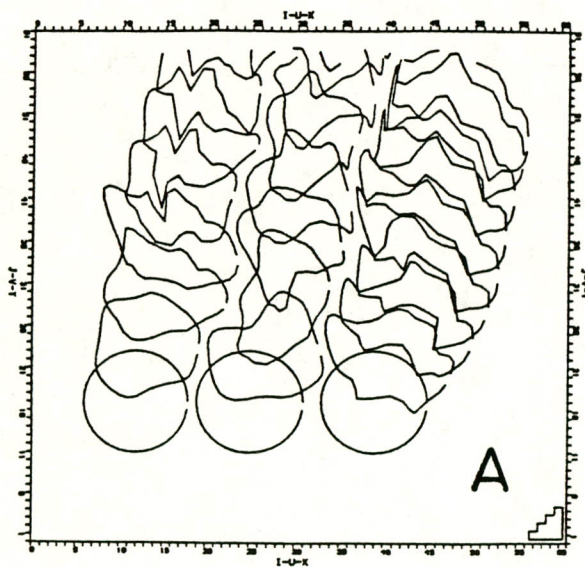


Fig. 6. Positions of the particle patches released in the relatively flat area A in the fine grid at intervals of 100 hrs between $T = 0$ and $T = 700$ (800) hrs

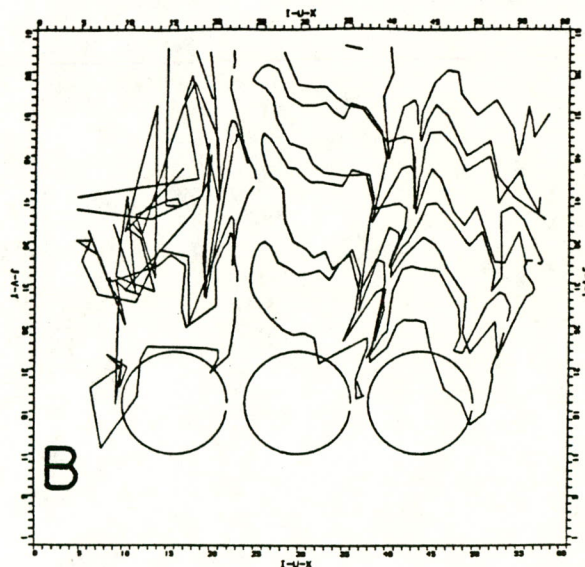


Fig. 7. Positions of the particle patches released in area B in the fine grid at intervals of 100 hrs between $T = 0$ and $T = 400$ hrs

areas B and B' with strong topographic features. The strongly distorted patches in Fig. 7 show that the fine grid velocity field is essentially different from the coarse grid velocity fields. The fine scale velocity structure effects the nature of the large scale transports. A simple smoothing of the patches now does not yield roughly the patches obtained in the coarse grid simulation.

In the simulation of spreading on large spatial and time scales essential information may apparently be lost if one uses velocity fields that are obtained in flow computations with too large a gridsize. In this context a grid-size is considered too large if important bottom topography details cannot be represented sufficiently, which leads to loss of fine velocity structure in the flow results, which in its turn affects the large scale spreading of matter.

On the basis of the above four experiments it may be concluded that in the Southern North Sea areas exist, where small scale bottom topography is important for the spreading of matter on large scales in space and time. If the proposed grid-size of the flow computation does not allow for a proper resolution of the topographic features, it may be necessary from an application point of view to parameterize its macroscopic effect in order to avoid grid dependence of the results. A further support for this conclusion can be found by repeating the particle track computations with a flow field that is obtained by averaging the fine grid flow field. This, however, is part of a different study and its results will be published elsewhere.

4 Application 2: Time-averaged velocity concepts and mean transports

In many studies interest is focussed on information about currents and transport of matter on large time scales, i.e. several months or longer. The problem of reducing the computational effort involved in simulating these large periods using a tidal model is an important one, see e.g. [4].

Well known concepts of tide-averaged (mean) velocities are the Eulerian residual velocity and the Eulerian residual transport velocity, defined by

$$\vec{u}_0(x, y, (t)) = \frac{1}{T} \int_{t-T/2}^{t+T/2} \vec{u}_1(x, y, t') dt' \quad (4.1)$$

and

$$\vec{u}_{0T}(x, y, (t)) = \frac{\frac{1}{T} \int_{t-T/2}^{t+T/2} \vec{u}_1 \{H(x, y) + \zeta(x, y, t')\} dt'}{\frac{1}{T} \int_{t-T/2}^{t+T/2} \{H(x, y) + \zeta(x, y, t')\} dt'} \quad (4.2)$$

respectively. T denotes the main tidal period or some larger cyclic flow period, while \vec{u}_1 , H , and ζ represent the tidal flow vector, depth below mean surface, and surface elevation, respectively. In [3], horizontal distributions of \vec{u}_0 and \vec{u}_{0T} in the North Sea are given for various flow situations of tide and tide plus wind. The problem in applying these time-averaged velocities in long term transport computations is their Eulerian nature, while particle motion is a Lagrangian concept.

In [2], van Dam suggests to use a different mean velocity, which meets this objection. This Lagrangian mean velocity is based on the net advective displacement of a particle during a tidal cycle T :

$$\begin{aligned} \vec{u}_{0L}(\vec{X}, t) &= \frac{1}{T} \{ \vec{X}(t + \frac{T}{2}) - \vec{X}(t - \frac{T}{2}) \} = \\ &= \frac{1}{T} \int_{t-T/2}^{t+T/2} \vec{u}_L(\vec{X}(t'), t') dt' \end{aligned} \quad (4.3)$$

For the case of mean tidal flow (cyclic forcing; $T=24.50$ hrs) plus an average winter wind state the mean velocities \vec{u}_0 , \vec{u}_{0T} , and \vec{u}_{0L} were determined in all grid points of an extended coarse grid model of the North Sea, see Figs. 8, 9 and 10.

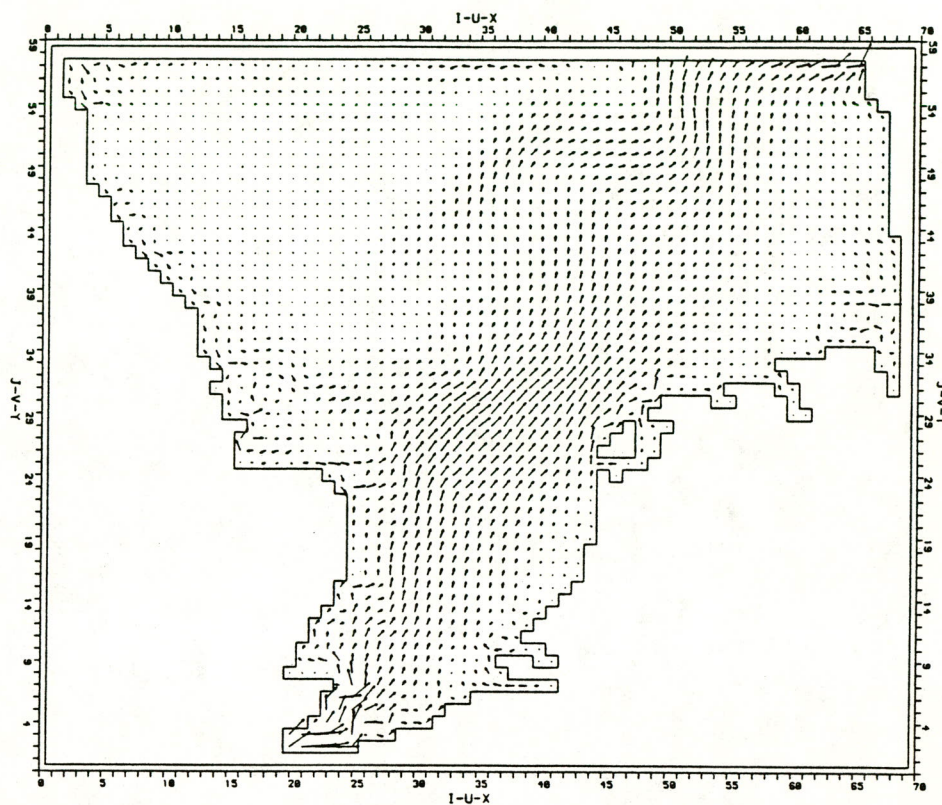


Fig. 8. Eulerian residual velocity field from a 10.000 m North Sea model

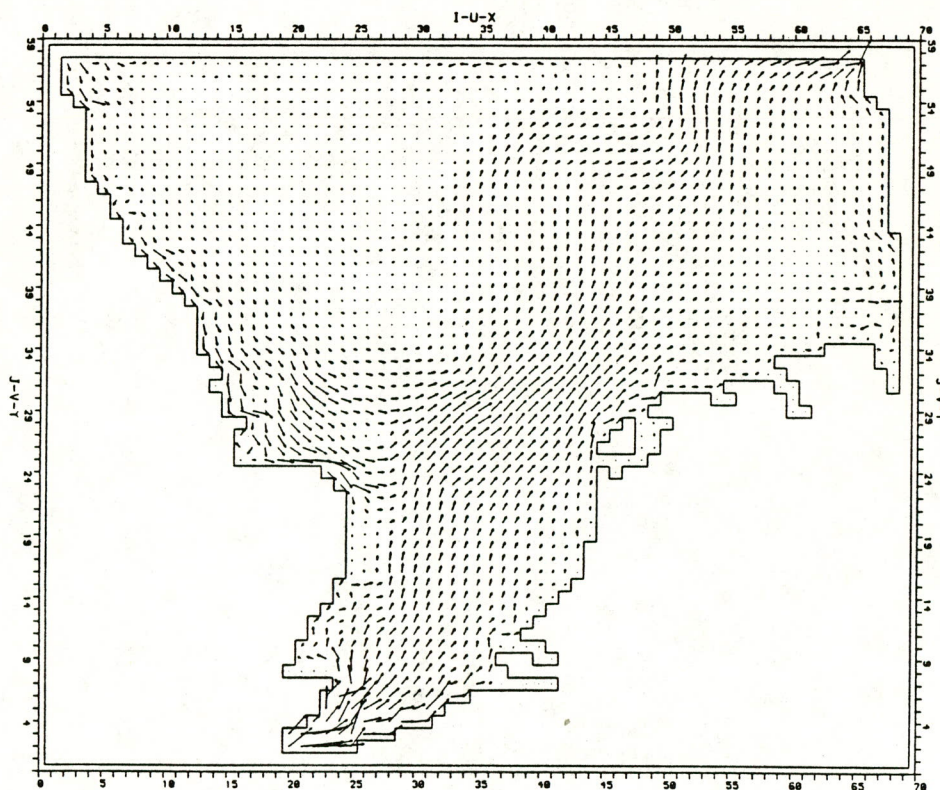


Fig. 9. Eulerian residual transport velocity field

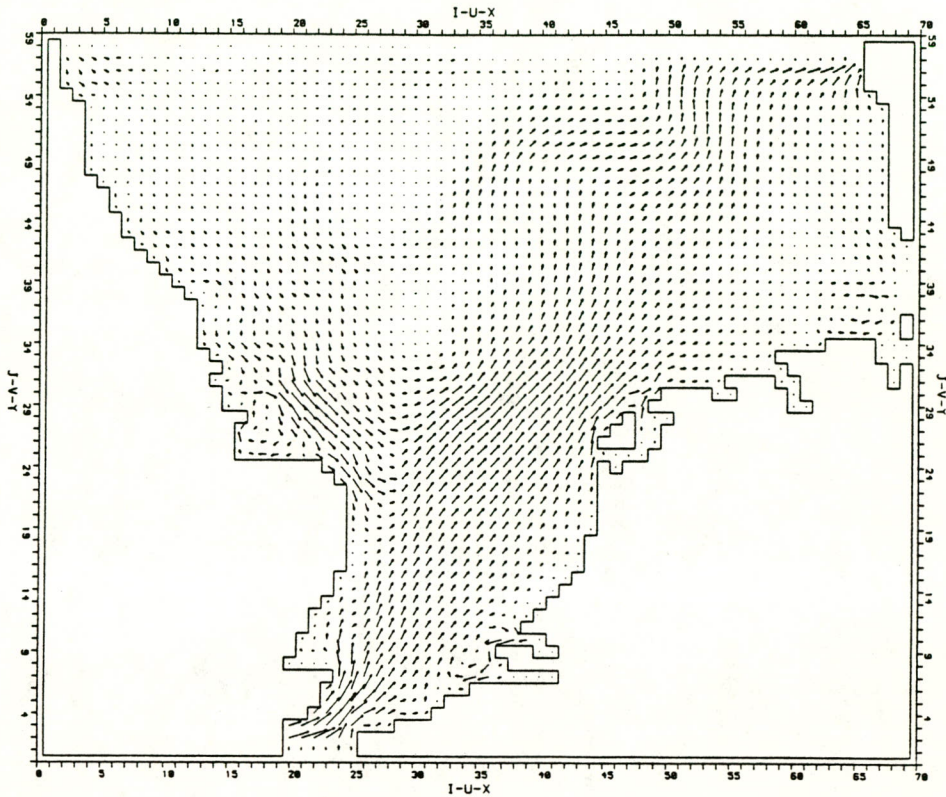


Fig. 10. Mean track velocity field

Although the general picture is similar for the three cases, there are remarkable and significant differences in the coastal areas, see e.g. the straight coastal areas along the English coast. Near the Southern boundary the mean track velocity field shows the most regular pattern of the three. It clearly contains two eddies in front of the Eastern and Western Scheldt entrances, with southward velocity directions immediately along the coast. This agrees with the results of Postma, [6], who found that particles released near the coast in that area tend to travel south, while the mean transport direction (Fig. 9) is north. The eddies can be explained from the combined effect of bottom topography variations and tidal pumping of the flow in the Scheldt estuaries, with the phase differences in longshore and inshore velocities playing a determinative role, see [6].

Three particle track simulations were performed to investigate the applicability of these mean velocities in the computation of long term advective transport of matter. An additional simulation using tidal velocities was made

to obtain a standard for comparison and evaluation. In all four simulations three circular patches were released in the Southern North Sea, each consisting of 40 particles distributed uniformly on the circle circumference. The subsequent particle positions were determined by solving Eq. 2.1 in a simulation which covered a period of 1500 hours.

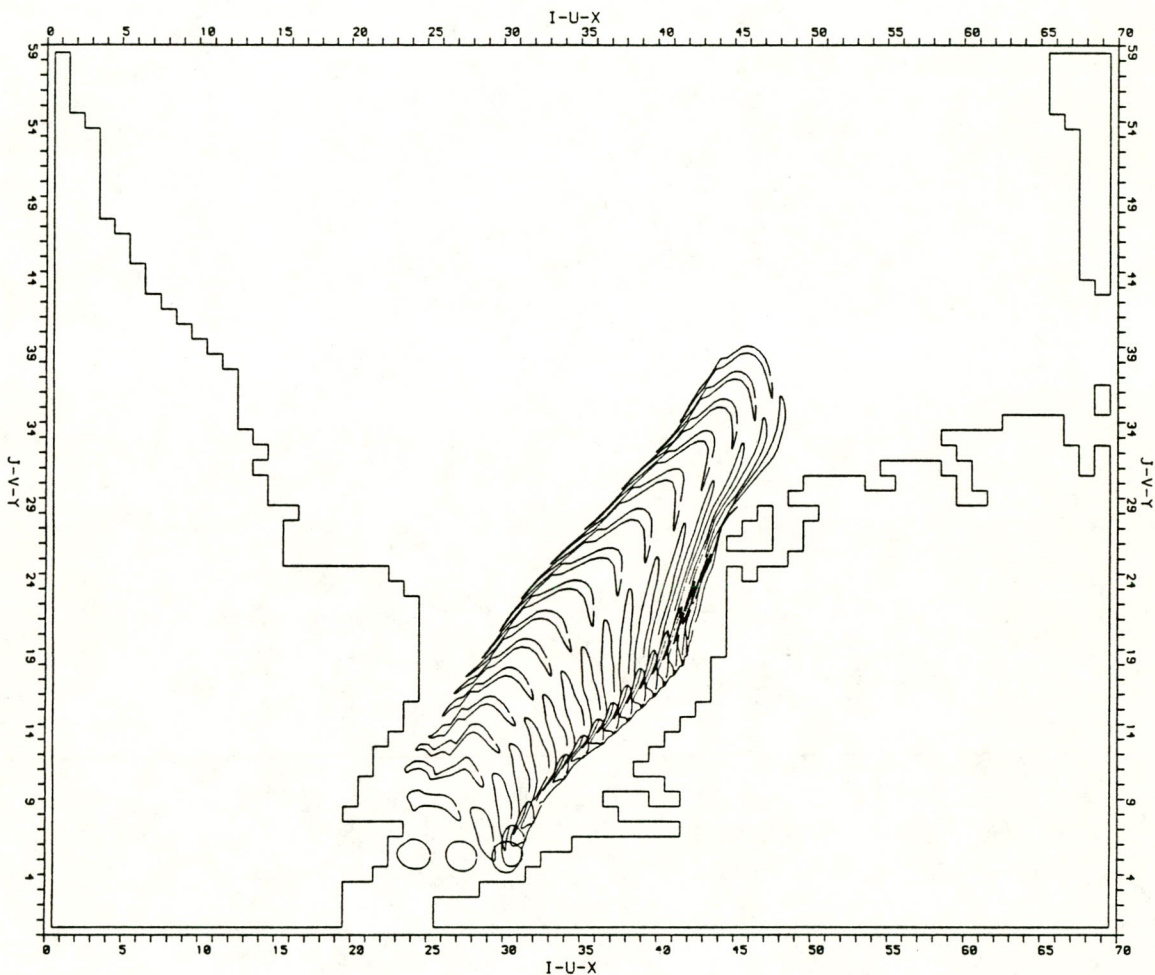


Fig. 11. Positions of particle patches determined using a cyclic tidal velocity field between $T = 0$ and $T = 1500$ hrs, at intervals of 100 hrs

Figs. 11-14 show the results in the form of patch boundaries at intervals of 100 hours. Comparing Figs. 12 and 13 with Fig. 11 it is apparent that the Eulerian residual transport velocity gives somewhat better results than the simple Eulerian residual velocity: the patches move more closely along the Dutch coast. In both cases, however, the individual patch displacements differ

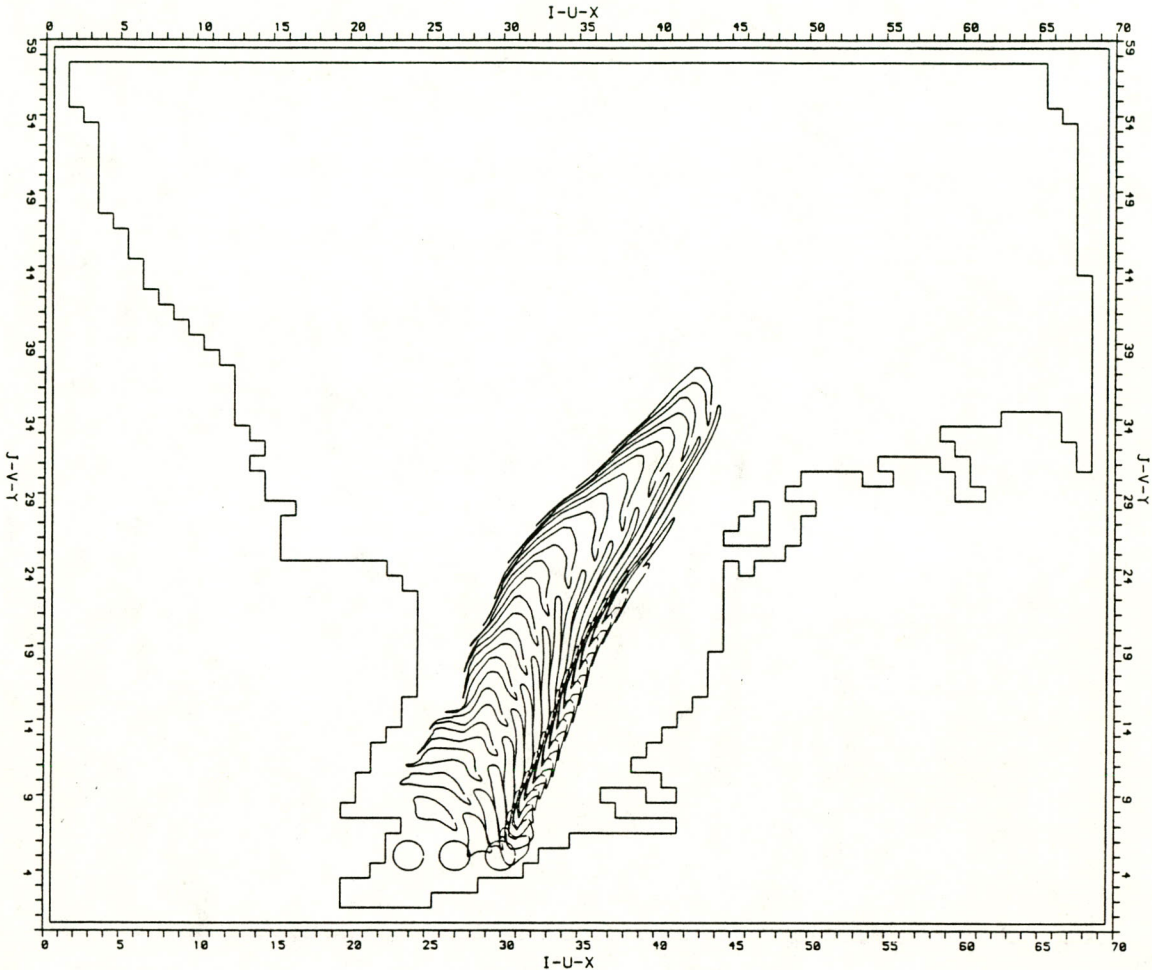


Fig. 12. As Fig. 11, but using the Eulerian residual velocity field

essentially from the ones computed with tidal velocities (Fig. 11). Fig. 14 on the other hand gives proof that the mean track velocity \vec{u}_0 can be a very accurate mean velocity concept in long term transport simulations in the North Sea. Both the envelope of the patches and the individual patches in Figs. 11 and 14 are quite similar. The minor differences that still exist are due to the fact that the mean track velocity does not contain the intra-tidal velocity fluctuation explicitly, but in integrated form. In nature, natural diffusion may well give rise to variations of this size and structure. It is therefore justified to represent these variations through some additional

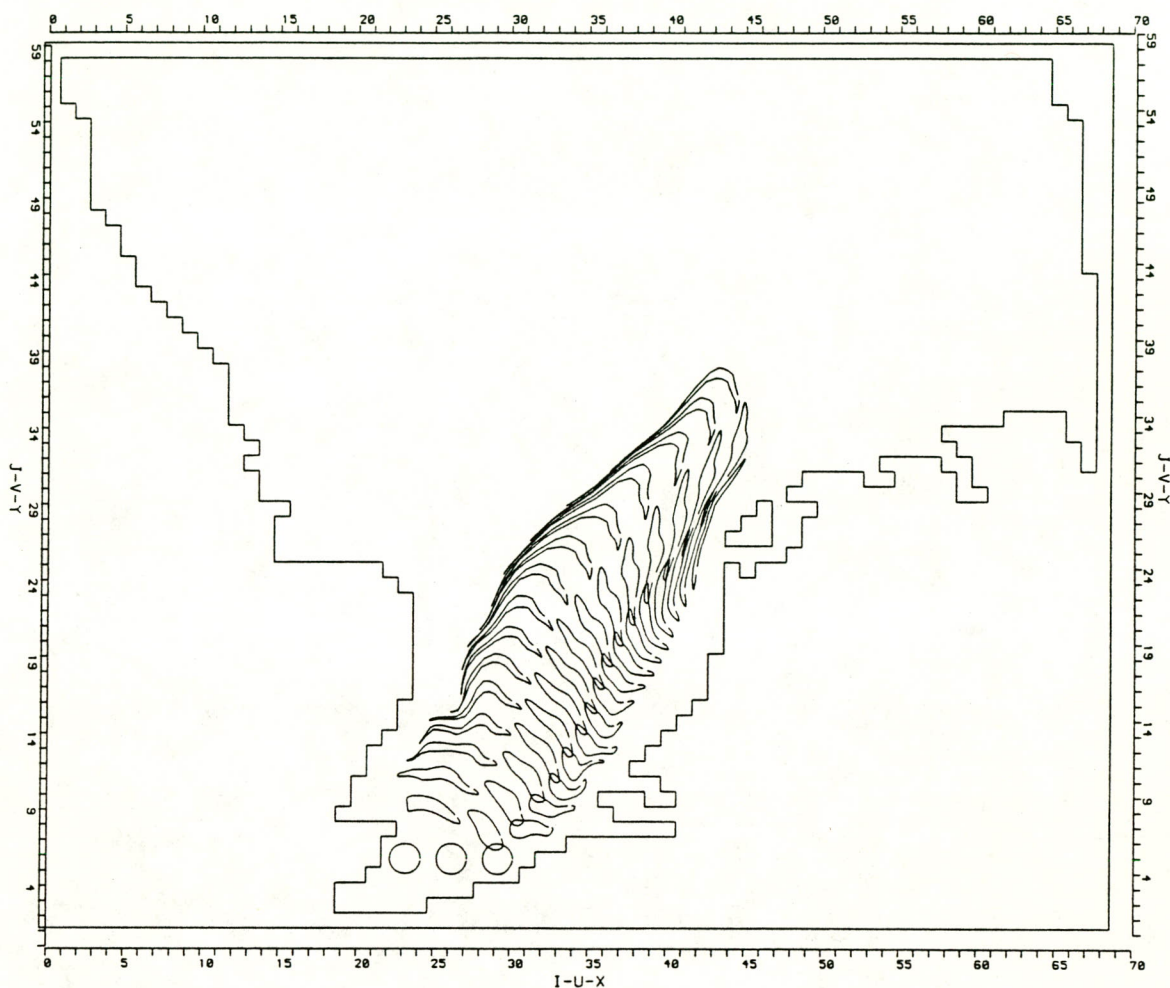


Fig. 13. As Fig. 11, but using the Eulerian residual transport velocity field

diffusion, when long-term transport computations using mean track velocities for the representation of the advective flow field are performed.

The agreement between the particle track results obtained using a mean track velocity field and those obtained using tidal velocities cannot be generalized to arbitrary situations and all types of simulations. In areas with large spatial variations in the flow the mean track velocity concept Eq. 4.3 is not uniquely defined any more, even in case of a fully cyclic tide. For large ratio of tidal excursion over gridsize the mean track velocity found applying Eq. 4.3 may strongly depend on the tidal phase t . This is for instance the case in many estuaries.

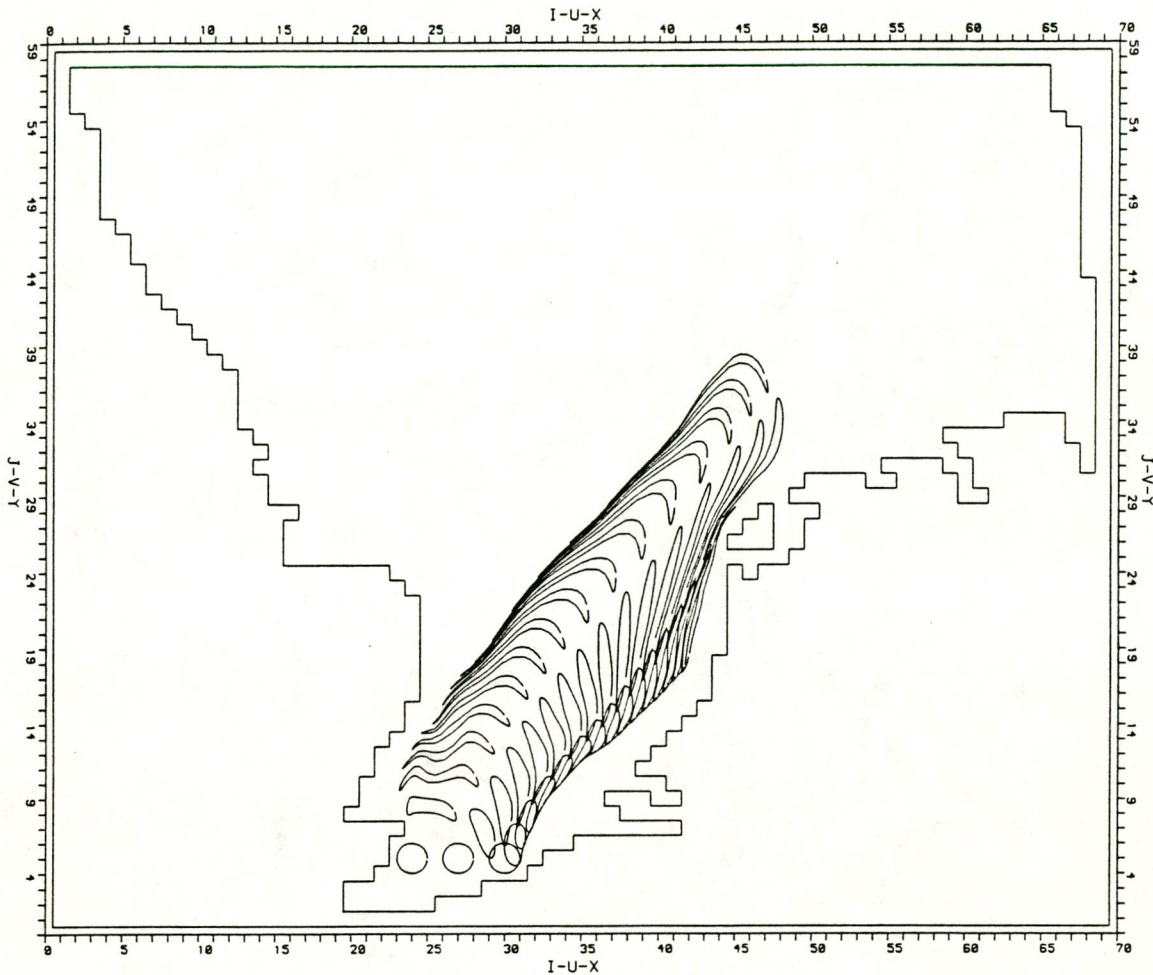


Fig. 14. As Fig. 11, but using the mean track velocity field

For the North Sea basin and the simulations presented, with the said ratio smaller than one, the tidal phase dependence of the mean track velocity is small; it is expected that its effect may be accounted for by some additional physically realistic diffusion.

A related complication is the introduction of particles at different phases. In case a mean track velocity field is used, this distribution in time has first to be translated into a corresponding initial distribution.

Both applications show, however, that a particle track computation model is a flexible and useful tool in many numerical investigations.

5 Conclusions

Some concluding remarks can be made

- A particle track simulation model is a quick and useful tool in the simulation of transport of passive matter. A modular structure simplifies the inclusion of a diffusive contribution and enhances the overall flexibility.
- Simple bilinear interpolation between grid points in the discrete velocity field restricts the formal accuracy of the solution of the differential equation for the particle displacement to first order. Further investigation of the interpolation procedure may be needed.
- Particle track computations give a much better insight in the quality and nature of velocity fields (e.g. residual flow fields) than the information provided by vector plots or velocity time histories.
- the Southern North Sea contains areas, where small scale bottom topography may play an important role in the spreading of matter on large scales in space and time.
- In cases that flow results from a numerical model are considered for use in long term transport simulations, it is important to know whether the essential topographic features of the area were resolved by the grid. Insufficient resolution leads to loss of the fine structure in the velocity field, which has bearing on the representation of the large scale transport of matter. From an application point of view a parameterization of its macroscopic effect may then be necessary to avoid grid dependence of the transport simulation results.
- The important small scale structure of the bottom topography in certain areas of the Southern North Sea is not sufficiently resolved in numerical models with gridsizes of order 10,000 m.
- Compared to the Eulerian residual velocity and the Eulerian residual transport velocity, the (Lagrangian) mean track velocity may both be an efficient and accurate concept of mean advective velocity in long term transport simulations in the North Sea.

References

1. Abraham, G, and Lindijer, G.J.H.
Physical/numerical investigation on the parameterization of turbulence and circulation phenomena in connection with water quality modelling of the North Sea.
Delft Hydraulics Laboratory, Report R 1920-I, 1984.
2. Dam, G.C. van
Reststromen en resttransport in modelberekeningen.
Rijkswaterstaat, Konzeptnota FA 8402, 1984.
3. Gerritsen, H.
Residual currents.
Delft Hydraulics Laboratory, Report R 1469-III, 1983.
4. Gerritsen, H.
Residual currents; a comparison of two modelling approaches.
In: Lecture Notes on coastal and estuarine studies.
Springer Verlag, in press (1985).
5. Leendertse, J.J.
Aspects of a computational model for long-period water-wave propagation.
Santa Monica, The Rand Corporation, Report RM-5294-PR, 1967.
6. Postma, L.
Enige bijzondere aspecten van het stoftransport langs de Zuid-Nederlandse Noordzeekust. (dit colloquium).

p.o. box 177

2600 mh delft

the netherlands